Forest Change Analysis by means of Pol-InSAR Measurements at L- and P-band

Noelia Romero-Puig[a], Matteo Pardini[a], Konstantinos P. Papathanassiou[a]
[a] German Aerospace Center (DLR), Microwaves and Radar Institute (HR), 82234 Wessling, Germany

Abstract

This work focuses on the detection and interpretation of forest structural changes by exploiting jointly polarimetric and interferometric SAR (Pol-InSAR) acquisitions. Using Pol-InSAR measurements and following a two-layer model assumption, the response from the forest canopy can be first decomposed into a ground and a volume layer. Then, a polarimetric change analysis can be applied over the separated ground and volume scattering components acquired at different times. The analysis of the detection and interpretation of the type of forest (structural) changes is carried out by exploiting L- and P-band data acquired by DLR's F-SAR sensor over the Traunstein forest in the context of the TMPSAR campaign. The results corroborate that the decomposition of the forest into simpler layers eases the interpretation of the changes.

1 Introduction

Different techniques that evaluate changes by means of polarimetric SAR (PolSAR) [1] acquisitions can be found [2, 3] in the literature. However, most of these techniques focus on detecting the amount of change in the backscattered intensity (i.e., radiometric information) between two acquisitions. In [4], a PolSAR change analysis technique that aims to provide an interpretation of the type of scattering mechanisms, associated with the type of changes, is introduced. It is based on the optimized contrast ratio [5, 6]. This methodology proposes a representation of the changes based on the type of change (scattering mechanisms) weighted by the amount of change (increasing/decreasing backscattered intensity).

Natural forests scenes are complex scattering scenarios from the radar point of view. This means that only with polarimetric acquisitions, the ambiguities arising from the superposition of structural and weather or seasonal changes cannot be resolved. A way to provide sensitivity to the vertical structure of the forest and overcome some of these ambiguities is by exploiting both polarimetric and interferometric SAR (Pol-InSAR) [7] measurements. Today, the potential and limitations of Pol-InSAR data for the reconstruction forest structural parameters are well understood. Yet, the question of how to qualitatively and quantitatively characterize forest change using Pol-InSAR data is, besides first attempts [8, 9], far from answered.

In this paper, forest changes are addressed by polarimetric change analysis on individual scattering contributions decomposed by means of Pol-InSAR techniques.

2 Forest Change Analysis Methods

2.1 PolSAR Change Analysis

Polarimetric SAR [1] acquisitions can be expressed in terms of the coherency matrix:

$$\mathbf{T} = \langle \mathbf{k}\mathbf{k}^H \rangle_N = \frac{1}{N}\sum_{n=1}^{N} \mathbf{k}_n \mathbf{k}_n^H. \qquad (1)$$

$\langle\cdot\rangle$ denotes spatial averaging (multi-looking), $\mathbf{k}_n$ is the Pauli scattering vector, and N is the number of samples used in the multi-looking window.

The change detection between two PolSAR images acquired over the same area at different acquisitions times is based on the associated coherency matrices $\mathbf{T}_1$ and $\mathbf{T}_2$. The power ratio between the two coherency matrices, known as the polarimetric contrast at a given polarization state $\mathbf{w}$, is defined as [5, 6]:

$$P_c(\mathbf{T}_1, \mathbf{T}_2, \mathbf{w}) = \frac{\mathbf{w}^H \mathbf{T}_2 \mathbf{w}}{\mathbf{w}^H \mathbf{T}_1 \mathbf{w}}. \qquad (2)$$

P_c is always real and positive. An increase in the backscattered power from $\mathbf{T}_1$ to $\mathbf{T}_2$ at the polarization state $\mathbf{w}$ is represented as $1 < P_c < \infty$, whereas a decrease is indicated as $0 < P_c < 1$. In absence of change, $P_c = 1$.

By optimizing (2), the maximum polarimetric contrast between acquisitions $\mathbf{T}_1$ and $\mathbf{T}_2$ can be obtained. This results in the following generalized eigenvalue decomposition [5]:

$$\mathbf{T}_2\mathbf{w} = \lambda \mathbf{T}_1 \mathbf{w}, \qquad (3)$$

with

$$|\mathbf{T}_2 - \lambda \mathbf{T}_1| = 0. \qquad (4)$$

The solution of (3) and (4) yields a set of three generalized eigenvalues (λ_i) and three corresponding generalized eigenvectors ($\mathbf{w}_i$). Sorted in descending order, i.e., $\lambda_1 \geq \lambda_2 \geq \lambda_3 > 0$, λ_1 represents the maximum polarimetric change (contrast) and λ_3 the minimum. The associated generalized eigenvectors (which are unitary, i.e. $\|\mathbf{w}_i\| = 1$) represent the polarization states at which the change (contrast) takes place.

The change information can be represented by means of the generalized eigenvalues and eigenvectors [4]. To this end, 3D real vectors $\mathbf{p}_{inc}$ and $\mathbf{p}_{dec}$ are formed from the generalized eigenvectors expressed in the Pauli basis and weighted by their associated eigenvalues. They correspond to the increasing ($\lambda_i > 1$) and decreasing ($\lambda_i < 1$) scattering contributions, respectively. These $\mathbf{p}_{inc}$ and $\mathbf{p}_{dec}$ are

then used to form Pauli RGB images, in which the intensity represents the amount of change and the colour the type of change. They are defined as follows:

$$\mathbf{p}_{inc} = \left[\sum_{i|\lambda_i>1}^{p} (10 \log_{10} \lambda_i)^2 \cdot \mathbf{w}_i \odot \mathbf{w}_i^* \right]^{\odot \frac{1}{2}}, \quad (5)$$

$$\mathbf{p}_{dec} = \left[\sum_{i|\lambda_i<1}^{p} (-10 \log_{10} \lambda_i)^2 \cdot \mathbf{w}_i \odot \mathbf{w}_i^* \right]^{\odot \frac{1}{2}}, \quad (6)$$

where $\odot$ represents the element by element product and $\mathbf{a}^{\odot 1/2}$ denotes the element by element square root of vector $\mathbf{a}$. It is worth mentioning that $\mathbf{p}_{inc}$ and $\mathbf{p}_{dec}$ are scaled in dB and, thus, the intensity of the increasing and decreasing images may be expressed in dB scale.

2.2 Pol-InSAR Change Analysis based on the Ground and Volume Components

The scattering complexity in forests yields a high polarimetric scattering entropy scenario. As a result, polarimetric information reduces, and the only information that remains available is interferometric information. One possibility to lower the entropy is to decompose the scattering processes into different scattering contributions and apply the polarimetric change analysis over the individual contributions. By using both polarimetric and interferometric acquisitions, the radar response from the forest canopy can be decomposed into ground and volume scattering components. This separation performs on the basis of the two-layer Random Volume over Ground (RVoG) [7] model.

According to this model, the complex interferometric coherence between two acquisitions (i.e., $i = 1$, $j = 2$) at a polarization state $\mathbf{w}$ can be expressed as:

$$\gamma_{ij}(\mathbf{w}) = \frac{\mathbf{w}^H \mathbf{\Omega}_{ij} \mathbf{w}}{\sqrt{(\mathbf{w}^H \mathbf{T}_i \mathbf{w})(\mathbf{w}^H \mathbf{T}_j \mathbf{w})}} = \frac{\gamma_{ij}^v + \gamma_{ij}^g \mu(\mathbf{w})}{1 + \mu(\mathbf{w})}. \quad (7)$$

In (7), $\mathbf{T}_i$ and $\mathbf{T}_j$ correspond to the coherency matrices containing polarimetric information, as defined in (1), and $\mathbf{\Omega}_{ij}$ is a complex matrix containing the interferometric information. On the right-hand side of the equation, γ_{ij}^g and γ_{ij}^v correspond to the interferometric coherence of the ground and volume layers, respectively; and $\mu(\mathbf{w})$ is the ground-to-volume ratio.

From (7), and according to the RVoG model, the different polarimetric ($\mathbf{T}_i$) and interferometric ($\mathbf{\Omega}_{ij}$) matrices can be expressed in terms of the ground and volume layers as follows:

$$\mathbf{T}_i = \mathbf{T}_g + \mathbf{T}_v, \quad (8)$$

$$\mathbf{\Omega}_{ij} = \gamma_{ij}^g \mathbf{T}_g + \gamma_{ij}^v \mathbf{T}_v. \quad (9)$$

By exploiting Pol-InSAR acquisitions, the polarimetric change analysis described in Section 2.1 is carried out over the separated ground $\mathbf{T}_g$ and volume $\mathbf{T}_v$ components [10, 11].

3 First Results

The evaluation of the proposed Pol-InSAR change analysis methodology is performed over an area around the temperate forest of Froschham, located in the south-east of Germany. Data acquired by DLR's airborne F-SAR sensor in the framework of the TMPSAR campaign are used. This campaign covers several years for which fully polarimetric multi-baseline data are available. In particular, L-band data are available for the years 2017, 2021, 2022 and 2023. P-band data are available for the years 2021, 2022 and 2023. A visualization of the SAR data acquired over the test site is provided in **Figure 1**. Two RGB Pauli images in radar coordinates corresponding to an L-band (left) and a P-band (right) acquisitions in 2022 are shown.

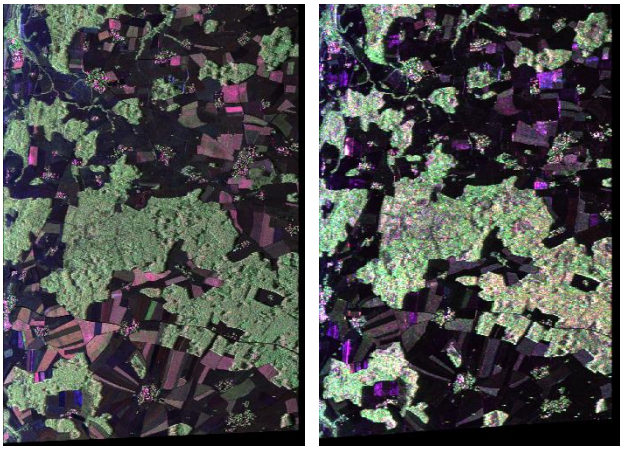

Figure 1 Pauli RGB images over the Froschham forest at L-band (left) and P-band (right) acquired on September 2022.

The fields around the forest, the majority of which are agricultural crops, appear in purple and dark colours. The forest itself, on the other hand, appears in greenish colours. This shows in both L- and P-band images.

The reference lidar data used for validation of the polarimetric change analysis is presented in **Figure 2**. It shows a height change map between the years 2018 and 2022, obtained from the reference lidar height H100 of each corresponding year. Non-forested areas are masked out in white. Some trends can be observed in the time span of four years. Clear cuts in which forest trees/stands have been removed show in dark blue colour. Other areas, such as the central part of the forest plot, show an increase of the forest height in the order of 2.5 to 5 m.

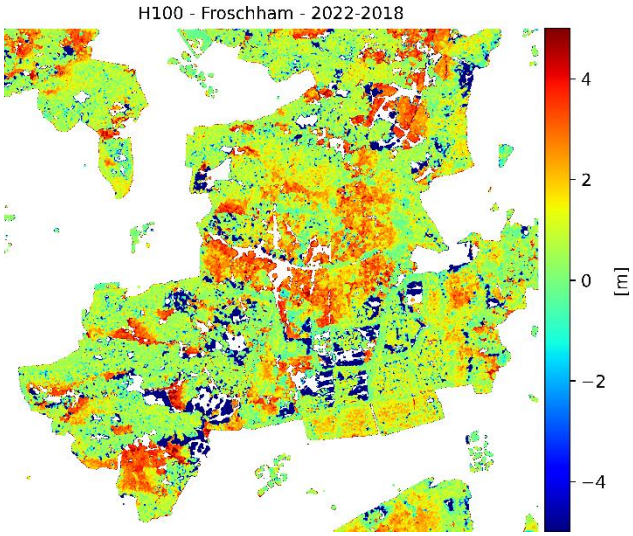

Figure 2 Lidar height change map over the Froschham forest between years 2018 and 2022. The map is derived from reference lidar height H100 at 5 m resolution.

The results of the PolSAR change analysis described in Section 2.1 are presented in **Figure 3**. To ease the interpretation, the results are geocoded so that a direct comparison with the reference lidar height map in **Figure 2** is possible. Two acquisitions with a one-year difference are selected, i.e., 2021 and 2022.

the scattering mechanisms. In addition, the changes are consistent in each of the frequency bands evaluated, i.e., L-band (top row) and P-band (bottom row). Both bands show in $\mathbf{p}_{dec}$ a decrease in the volume scattering component (in greenish colour) over the clear cuts observed in the lidar height change map.

The histograms of the eigenvalues demonstrate that the forest appears as a complex scenario to the radar. Three different eigenvalues, in which at least two show an average contribution above 0 dB, are present. The long wavelength of L- and P-band data, around 20 cm and 70 cm, respectively, allows the SAR signal to penetrate into and through the forest canopy and reach the ground. A ground scattering is therefore expected to be the dominant ground contribution, especially at P-band. This shows in **Figure 3 (f)**, where the first eigenvalue is of higher magnitude and more separated from the secondary ones.

The presence of a dominant ground scattering contribution in a still relatively high entropy scenario limits our capability to distinguish between more than one type of possible dominant scattering mechanisms. $\mathbf{p}_{inc}$ in **Figure 3 (d)** reflects this. As expected at P-band, the largest change appears to come from the ground component. This results in a purple colour over the forest, indicating a mix of dominant surface (HH+VV corresponds to the blue channel) and dihedral (HH-VV corresponds to the red channel) scattering mechanisms.

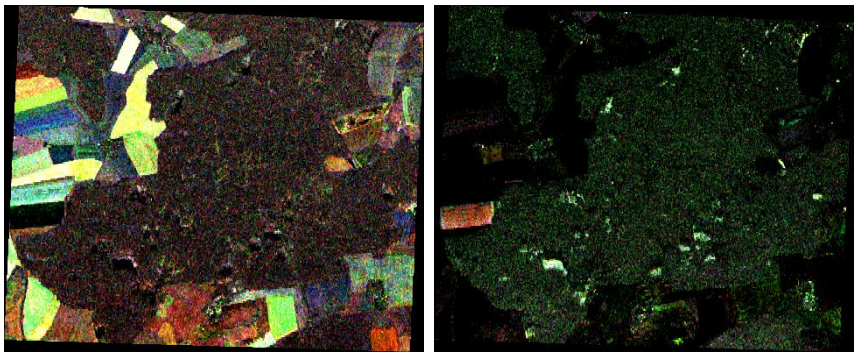

(a) $\boldsymbol{p}_{inc}$ at L-band.

(b) $\mathbf{p}_{dec}$ at L-band.

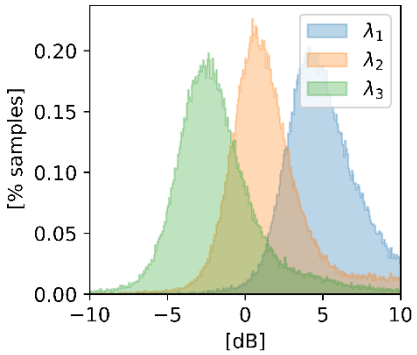

(c) Histogram of the eigenvalues at L-band.

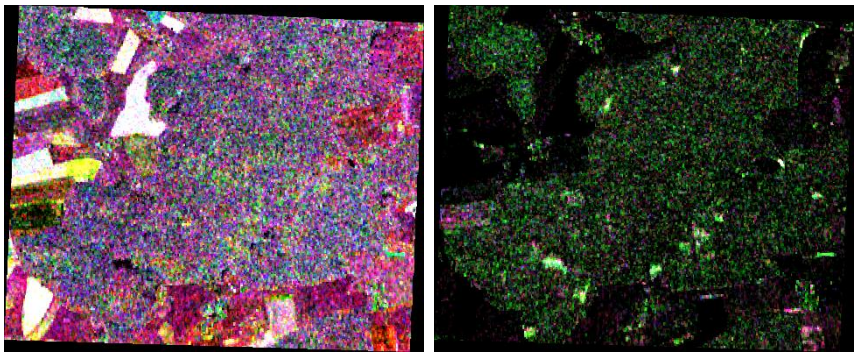

(d) $\boldsymbol{p}_{inc}$ at P-band.

(e) $\boldsymbol{p}_{dec}$ at P-band.

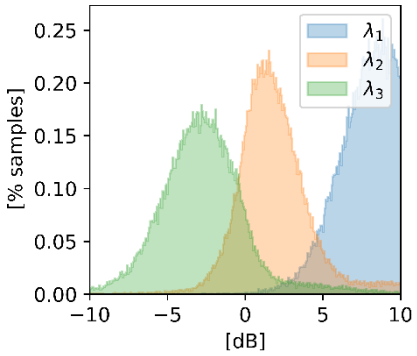

(f) Histogram of the eigenvalues at P-band.

Figure 3 PolSAR change analysis between two images acquired on 17 June 2021 and 22 September 2022 at L-band (first row) and P-band (second row). Azimuth and range resolution are 5 m x 5 m (ENL = 34) for L-band data, and 10 m x 10 m (ENL = 15) for P-band. From left to right, the increase and decrease power ratios of the changes, and the histogram of the generalized eigendecomposition are presented. The magnitude of the change is scaled from 1 to 10 dB.

The increase and decrease power ratios show changes in both the backscattering intensity and in the polarization, in

In order to better distinguish between the different types of

changes in the forest canopy, the PolSAR change analysis is applied over the ground and volume components, which have been separated by means of Pol-InSAR (see Section 2.2). The results are shown in **Figure 4** for the P-band case.

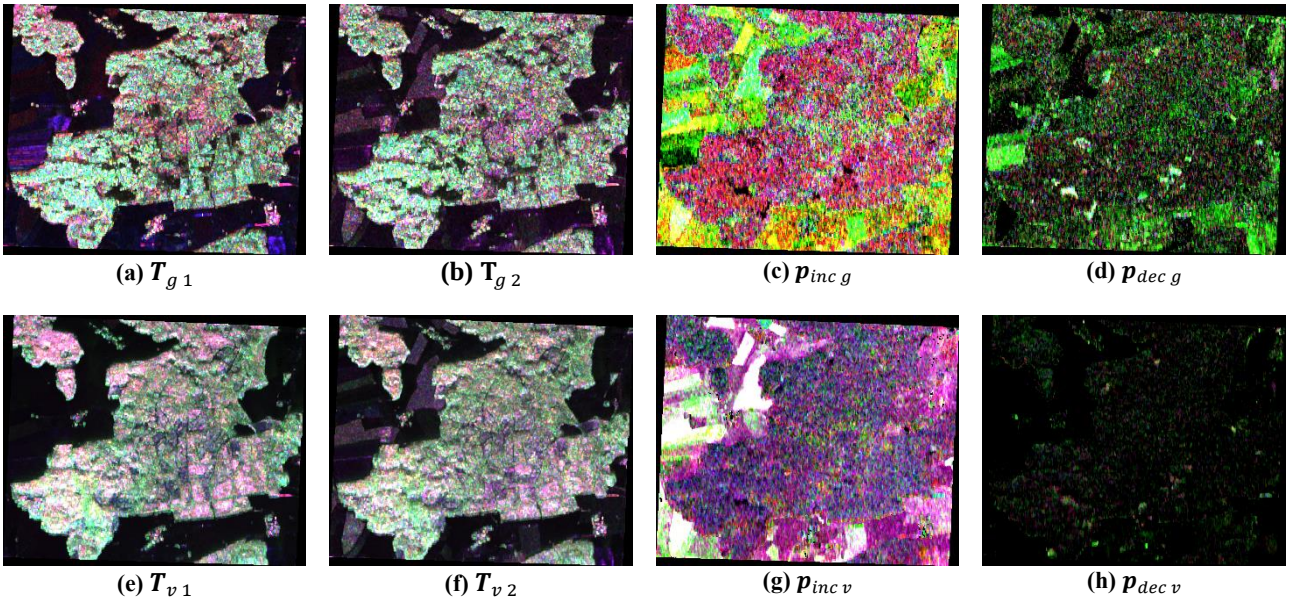

(a) $\boldsymbol{T}_{g\,1}$ **(b)** $\mathbf{T}_{g\,2}$ **(c)** $\boldsymbol{p}_{inc\,g}$ **(d)** $\boldsymbol{p}_{dec\,g}$

(e) $\boldsymbol{T}_{v\,1}$ **(f)** $\boldsymbol{T}_{v\,2}$ **(g)** $\boldsymbol{p}_{inc\,v}$ **(h)** $\boldsymbol{p}_{dec\,v}$

Figure 4 PolSAR change analysis over the ground and volume scattering components between acquisitions acquired on 2021 and 2022 at P-band. Azimuth and range resolution are around 30 m x 30 m (ENL = 132). From left to right, the separated ground and volume components ($\boldsymbol{T}_g$ and $\boldsymbol{T}_v$) of each acquisition, together with the increase and decrease power ratios of the changes, are presented. The magnitude of the change is scaled from 1 to 10 dB.

The polarimetric change analysis over the separated ground and volume components simplifies the interpretation of the type of changes occurring in the different layers of the forest canopy. The power ratios of the ground component indicate an increase of dihedral scattering (reddish colour in $\mathbf{p}_{inc\,g}$) over the forested areas. At the same time, in the central area of the forest, which show in pink in $\mathbf{T}_{g\,1}$ and $\mathbf{T}_{g\,2}$, an increase of the volume scattering contribution is observed. This shows in $\mathbf{p}_{inc\,g}$ and $\mathbf{p}_{dec\,g}$ in green, which is associated with the cross-pol channel. This is also visible in the power ratio of the volume component, $\mathbf{p}_{inc\,v}$. A visual qualitative evaluation with respect to the lidar height change map in **Figure 2** corroborates these observations. In that area, the forest has grown an average of 2.5 to 5 m.

4 Conclusions

The results of the proposed change analysis methodology by combining polarimetric and interferometric data have proven to be sensitive to structural changes in forests. As pointed out by the latest works addressing this topic [12, 13], the challenge remains, however, not in the detection of changes, but in their interpretation.

The comparison of the results at L- and P-band corroborate the complementary information provided by each frequency band. Nevertheless, the large wavelength of P-band data leads to a slightly lower entropy scenario thanks to a stronger ground scattering contribution than at L-band. This, in principle, is beneficial for the interpretation of the type of forest changes (type of scattering mechanisms) at P-band.

Exploiting polarimetric data alone limits the detection and interpretation of the changes in the forest structure. In an attempt to overcome this limitation and increase the sensitivity to the change processes, interferometry is introduced. With Pol-InSAR observations, the scattering from the forest can be decomposed into ground and volume scattering contributions. The results of the PolSAR change analysis over the separated ground and volume components show an increased dynamic range of detectable changes, which provides insights into the changes occurring in each layer. Conclusions derived from this work aim to advance the development of new applications for future missions, such as BIOMASS.

5 Literature

[1] S. Cloude, “Polarisation: Applications in Remote Sensing”. New York, NY, USA: Oxford Univ. Press, 2009.

[2] K. Conradsen, A. A. Nielsen, J. Schou, and H. Skriver, “A test statistic in the complex wishart distribution and its application to change detection in polarimetric SAR data,” IEEE Trans. Geosci. Remote Sens., vol. 41, no. 1, pp. 4–19, Jan. 2003.

[3] A. Marino, S. R. Cloude, and J. M. Lopez-Sanchez, “A new polarimetric change detector in radar imagery,” IEEE Trans. Geosci. Remote Sens., vol. 51, no. 5, pp. 2986–3000, May 2013.

[4] A. Alonso-González, C. López-Martínez, K. P. Papathanassiou and I. Hajnsek, “Polarimetric SAR Time Series Change Analysis Over Agricultural Areas,”

IEEE Trans. Geosci. and Remote Sens., vol. 58, no. 10, pp. 7317-7330, Oct. 2020.

[5] A. Kostinski and W. Boerner, "On the polarimetric contrast optimization," IEEE Trans. Antennas Propag., vol. 35, no. 8, pp. 988-991, Aug. 1987.

[6] A. Swartz, H. A. Yueh, J. A. Kong, L. M. Novak, and R. T. Shin, "Optimal polarizations for achieving maximum contrast in radar images", J. Geophys. Res., vol. 93(B12), pp. 15252–15260, Dec. 1998.

[7] K. P. Papathanassiou and S. R. Cloude, "Single-baseline polarimetric SAR interferometry," IEEE Trans. Geosci. and Remote Sens., vol. 39, no. 11, pp. 2352-2363, Nov. 2001.

[8] M. Tello, V. Cazcarra-Bes, M. Pardini and K. Papathanassiou, "Forest Structure Characterization from SAR Tomography at L-Band," IEEE J. Sel. Top. Appl. Earth Obs. Remote Sens., vol. 11, no. 10, pp. 3402-3414, Oct. 2018.

[9] V. Cazcarra-Bes, M. Pardini and K. Papathanassiou, "Definition of Tomographic SAR Configurations for Forest Structure Applications at L-Band," IEEE Geosci. Remote Sens. Lett., vol. 19, pp. 1-5, 2022.

[10] A. Alonso-González and K. P. Papathanassiou, "Multibaseline Two Layer Model PolInSAR Ground and Volume Separation," EUSAR 2018; 12th European Conference on Synthetic Aperture Radar, pp. 1-5. VDE, June 2018.

[11] Alonso-González, A., Papathanassiou, K. "Polarimetric Change Analysis in Forest using PolInSAR Ground and Volume separation techniques," EUSAR 2021; 13th European Conference on Synthetic Aperture Radar, pp. 1-6. VDE, 2021.

[12] S. Cloude, "A Physical Approach to POLSAR Time Series Change Analysis," IEEE Geosci. Remote Sens. Letters, vol. 19, pp. 1-4, 2022.

[13] A. Marino and M. Nannini, "Signal Models for Changes in Polarimetric SAR Data," IEEE Trans, Geosci. and Remote Sens., vol. 60, pp. 1-18, 2022.